Evidence for the h[subscript b](1P) meson in the decay #(3S)→π[superscript 0]h[subscript b](1P)

Citation: J. P. Lees et al. "Evidence for the h[subscript b](1P) meson in the decay Y(3S)→π[superscript 0]h[subscript b](1P)" Physical Review D 84, 091101(R)(2011). © 2011 American Physical Society

As Published: http://dx.doi.org/10.1103/PhysRevD.84.091101

Publisher: American Physical Society

Persistent URL: http://hdl.handle.net/1721.1/71208

Version: Final published version: final published article, as it appeared in a journal, conference proceedings, or other formally published context

Massachusetts Institute of Technology

Evidence for the $h_b(1P)$ meson in the decay $\Upsilon(3S) \to \pi^0 h_b(1P)$

J. P. Lees,[1] V. Poireau,[1] E. Prencipe,[1] V. Tisserand,[1] J. Garra Tico,[2] E. Grauges,[2] M. Martinelli,[3a,3b] D. A. Milanes,[3a,3b] A. Palano,[3a,3b] M. Pappagallo,[3a,3b] G. Eigen,[4] B. Stugu,[4] L. Sun,[4] D. N. Brown,[5] L. T. Kerth,[5] Yu. G. Kolomensky,[5] G. Lynch,[5] I. L. Osipenkov,[5] H. Koch,[6] T. Schroeder,[6] D. J. Asgeirsson,[7] C. Hearty,[7] T. S. Mattison,[7] J. A. McKenna,[7] A. Khan,[8] V. E. Blinov,[9] A. R. Buzykaev,[9] V. P. Druzhinin,[9] V. B. Golubev,[9] E. A. Kravchenko,[9] A. P. Onuchin,[9] S. I. Serednyakov,[9] Yu. I. Skovpen,[9] E. P. Solodov,[9] K. Yu. Todyshev,[9] A. N. Yushkov,[9] M. Bondioli,[10] S. Curry,[10] D. Kirkby,[10] A. J. Lankford,[10] M. Mandelkern,[10] D. P. Stoker,[10] H. Atmacan,[11] J. W. Gary,[11] F. Liu,[11] O. Long,[11] G. M. Vitug,[11] C. Campagnari,[12] T. M. Hong,[12] D. Kovalskyi,[12] J. D. Richman,[12] C. A. West,[12] A. M. Eisner,[13] J. Kroseberg,[13] W. S. Lockman,[13] A. J. Martinez,[13] T. Schalk,[13] B. A. Schumm,[13] A. Seiden,[13] C. H. Cheng,[14] D. A. Doll,[14] B. Echenard,[14] K. T. Flood,[14] D. G. Hitlin,[14] P. Ongmongkolkul,[14] F. C. Porter,[14] A. Y. Rakitin,[14] R. Andreassen,[15] M. S. Dubrovin,[15] B. T. Meadows,[15] M. D. Sokoloff,[15] P. C. Bloom,[16] W. T. Ford,[16] A. Gaz,[16] M. Nagel,[16] U. Nauenberg,[16] J. G. Smith,[16] S. R. Wagner,[16] R. Ayad,[17,*] W. H. Toki,[17] H. Jasper,[18] A. Petzold,[18] B. Spaan,[18] M. J. Kobel,[19] K. R. Schubert,[19] R. Schwierz,[19] D. Bernard,[20] M. Verderi,[20] P. J. Clark,[21] S. Playfer,[21] J. E. Watson,[21] D. Bettoni,[22a] C. Bozzi,[22a] R. Calabrese,[22a,22b] G. Cibinetto,[22a,22b] E. Fioravanti,[22a,22b] I. Garzia,[22a,22b] E. Luppi,[22a,22b] M. Munerato,[22a,22b] M. Negrini,[22a,22b] L. Piemontese,[22a] R. Baldini-Ferroli,[23] A. Calcaterra,[23] R. de Sangro,[23] G. Finocchiaro,[23] M. Nicolaci,[23] S. Pacetti,[23] P. Patteri,[23] I. M. Peruzzi,[23,†] M. Piccolo,[23] M. Rama,[23] A. Zallo,[23] R. Contri,[24a,24b] E. Guido,[24a,24b] M. Lo Vetere,[24a,24b] M. R. Monge,[24a,24b] S. Passaggio,[24a] C. Patrignani,[24a,24b] E. Robutti,[24a] B. Bhuyan,[25] V. Prasad,[25] C. L. Lee,[26] M. Morii,[26] A. J. Edwards,[27] A. Adametz,[1] J. Marks,[1] U. Uwer,[1] F. U. Bernlochner,[29] M. Ebert,[29] H. M. Lacker,[29] T. Lueck,[29] P. D. Dauncey,[30] M. Tibbetts,[30] P. K. Behera,[31] U. Mallik,[31] C. Chen,[32] J. Cochran,[32] H. B. Crawley,[32] W. T. Meyer,[32] S. Prell,[32] E. I. Rosenberg,[32] A. E. Rubin,[32] A. V. Gritsan,[33] Z. J. Guo,[33] N. Arnaud,[2] M. Davier,[2] D. Derkach,[2] J. Firmino da Costa,[2] G. Grosdidier,[2] F. Le Diberder,[2] A. M. Lutz,[2] B. Malaescu,[2] A. Perez,[2] P. Roudeau,[2] M. H. Schune,[2] A. Stocchi,[2] L. Wang,[2] G. Wormser,[2] D. J. Lange,[35] D. M. Wright,[35] I. Bingham,[36] C. A. Chavez,[36] J. P. Coleman,[36] J. R. Fry,[36] E. Gabathuler,[36] D. E. Hutchcroft,[36] D. J. Payne,[36] C. Touramanis,[36] A. J. Bevan,[37] F. Di Lodovico,[37] R. Sacco,[37] M. Sigamani,[37] G. Cowan,[38] S. Paramesvaran,[38] A. C. Wren,[38] D. N. Brown,[39] C. L. Davis,[39] A. G. Denig,[3] M. Fritsch,[3] W. Gradl,[3] A. Hafner,[3] K. E. Alwyn,[41] D. Bailey,[41] R. J. Barlow,[41] G. Jackson,[41] G. D. Lafferty,[41] R. Cenci,[42] B. Hamilton,[42] A. Jawahery,[42] D. A. Roberts,[42] G. Simi,[42] C. Dallapiccola,[43] E. Salvati,[43] R. Cowan,[44] D. Dujmic,[44] G. Sciolla,[44] D. Lindemann,[45] P. M. Patel,[45] S. H. Robertson,[45] M. Schram,[45] P. Biassoni,[46a,46b] A. Lazzaro,[46a,46b] V. Lombardo,[46a] F. Palombo,[46a,46b] S. Stracka,[46a,46b] L. Cremaldi,[47] R. Godang,[47,‡] R. Kroeger,[47] P. Sonnek,[47] D. J. Summers,[47] X. Nguyen,[4] P. Taras,[4] G. De Nardo,[49a,49b] D. Monorchio,[49a,49b] G. Onorato,[49a,49b] C. Sciacca,[49a,49b] G. Raven,[50] H. L. Snoek,[50] C. P. Jessop,[51] K. J. Knoepfel,[51] J. M. LoSecco,[51] W. F. Wang,[51] L. A. Corwin,[52] K. Honscheid,[52] R. Kass,[52] N. L. Blount,[53] J. Brau,[53] R. Frey,[53] J. A. Kolb,[53] R. Rahmat,[53] N. B. Sinev,[53] D. Strom,[53] J. Strube,[53] E. Torrence,[53] G. Castelli,[54a,54b] E. Feltresi,[54a,54b] N. Gagliardi,[54a,54b] M. Margoni,[54a,54b] M. Morandin,[54a] M. Posocco,[54a] M. Rotondo,[54a] F. Simonetto,[54a,54b] R. Stroili,[54a,54b] E. Ben-Haim,[55] M. Bomben,[55] G. R. Bonneaud,[55] H. Briand,[55] G. Calderini,[55] J. Chauveau,[55] O. Hamon,[55] Ph. Leruste,[55] G. Marchiori,[55] J. Ocariz,[55] S. Sitt,[55] M. Biasini,[56a,56b] E. Manoni,[56a,56b] A. Rossi,[56a,56b] C. Angelini,[57a,57b] G. Batignani,[57a,57b] S. Bettarini,[57a,57b] M. Carpinelli,[57a,57b,§] G. Casarosa,[57a,57b] A. Cervelli,[57a,57b] F. Forti,[57a,57b] M. A. Giorgi,[57a,57b] A. Lusiani,[57a,57c] N. Neri,[57a,57b] E. Paoloni,[57a,57b] G. Rizzo,[57a,57b] J. J. Walsh,[57a] D. Lopes Pegna,[58] C. Lu,[58] J. Olsen,[58] A. J. S. Smith,[58] A. V. Telnov,[58] F. Anulli,[59a] G. Cavoto,[59a] R. Faccini,[59a,59b] F. Ferrarotto,[59a] F. Ferroni,[59a,59b] M. Gaspero,[59a,59b] L. Li Gioi,[59a] M. A. Mazzoni,[59a] G. Piredda,[59a] C. Bünger,[60] T. Hartmann,[60] T. Leddig,[60] H. Schröder,[60] R. Waldi,[60] T. Adye,[61] E. O. Olaiya,[61] F. F. Wilson,[61] S. Emery,[62] G. Hamel de Monchenault,[62] G. Vasseur,[62] Ch. Yèche,[62] M. T. Allen,[63] D. Aston,[63] D. J. Bard,[63] R. Bartoldus,[63] J. F. Benitez,[63] C. Cartaro,[63] M. R. Convery,[63] J. Dorfan,[63] G. P. Dubois-Felsmann,[63] W. Dunwoodie,[63] R. C. Field,[63] M. Franco Sevilla,[63] B. G. Fulsom,[63] A. M. Gabareen,[63] M. T. Graham,[63] P. Grenier,[63] C. Hast,[63] W. R. Innes,[63] M. H. Kelsey,[63] H. Kim,[63] P. Kim,[63] M. L. Kocian,[63] D. W. G. S. Leith,[63] P. Lewis,[63] S. Li,[63] B. Lindquist,[63] S. Luitz,[63] V. Luth,[63] H. L. Lynch,[63] D. B. MacFarlane,[63] D. R. Muller,[63] H. Neal,[63] S. Nelson,[63] C. P. O'Grady,[63] I. Ofte,[63] M. Perl,[63] T. Pulliam,[63] B. N. Ratcliff,[63] S. H. Robertson,[63] A. Roodman,[63] A. A. Salnikov,[63] V. Santoro,[63] R. H. Schindler,[63] J. Schwiening,[63] A. Snyder,[63] D. Su,[63] M. K. Sullivan,[63] S. Sun,[63] K. Suzuki,[63] J. M. Thompson,[63] J. Va'vra,[63] A. P. Wagner,[63] M. Weaver,[63] W. J. Wisniewski,[63] M. Wittgen,[63] D. H. Wright,[63] H. W. Wulsin,[63] A. K. Yarritu,[63] C. C. Young,[63] V. Ziegler,[63] X. R. Chen,[64] W. Park,[64] M. V. Purohit,[64] R. M. White,[64] J. R. Wilson,[64] A. Randle-Conde,[65] S. J. Sekula,[65] M. Bellis,[66] P. R. Burchat,[66] T. S. Miyashita,[66] M. S. Alam,[67] J. A. Ernst,[67] N. Guttman,[68] A. Soffer,[68]

091101-1

P. Lund,[69] S. M. Spanier,[69] R. Eckmann,[70] J. L. Ritchie,[70] A. M. Ruland,[70] C. J. Schilling,[70] R. F. Schwitters,[70] B. C. Wray,[70] J. M. Izen,[71] X. C. Lou,[71] F. Bianchi,[72a,72b] D. Gamba,[72a,72b] M. Pelliccioni,[72a,72b] L. Lanceri,[73a,73b] L. Vitale,[73a,73b] N. Lopez-March,[74] F. Martinez-Vidal,[74] A. Oyanguren,[74] H. Ahmed,[75] J. Albert,[75] Sw. Banerjee,[75] H. H. F. Choi,[75] K. Hamano,[75] G. J. King,[75] R. Kowalewski,[75] M. J. Lewczuk,[75] C. Lindsay,[75] I. M. Nugent,[75] J. M. Roney,[75] R. J. Sobie,[75] T. J. Gershon,[76] P. F. Harrison,[76] T. E. Latham,[76] E. M. T. Puccio,[76] H. R. Band,[77] S. Dasu,[77] Y. Pan,[77] R. Prepost,[77] C. O. Vuosalo,[77] and S. L. Wu[77]

(The *BABAR* Collaboration)

[1]*Laboratoire d'Annecy-le-Vieux de Physique des Particules (LAPP), Université de Savoie, CNRS/IN2P3, F-74941 Annecy-Le-Vieux, France*
[2]*Universitat de Barcelona, Facultat de Fisica, Departament ECM, E-08028 Barcelona, Spain*
[3a]*INFN Sezione di Baria, I-70126 Bari, Italy*
[3b]*Dipartimento di Fisica, Università di Barib, I-70126 Bari, Italy*
[4]*University of Bergen, Institute of Physics, N-5007 Bergen, Norway*
[5]*Lawrence Berkeley National Laboratory and University of California, Berkeley, California 94720, USA*
[6]*Ruhr Universität Bochum, Institut für Experimentalphysik 1, D-44780 Bochum, Germany*
[7]*University of British Columbia, Vancouver, British Columbia, Canada V6T1 Z1*
[8]*Brunel University, Uxbridge, Middlesex UB8 3 PH, United Kingdom*
[9]*Budker Institute of Nuclear Physics, Novosibirsk 630090, Russia*
[10]*University of California at Irvine, Irvine, California 92697, USA*
[11]*University of California at Riverside, Riverside, California 92521, USA*
[12]*University of California at Santa Barbara, Santa Barbara, California 93106, USA*
[13]*University of California at Santa Cruz, Institute for Particle Physics, Santa Cruz, California 95064, USA*
[14]*California Institute of Technology, Pasadena, California 91125, USA*
[15]*University of Cincinnati, Cincinnati, Ohio 45221, USA*
[16]*University of Colorado, Boulder, Colorado 80309, USA*
[17]*Colorado State University, Fort Collins, Colorado 80523, USA*
[18]*Technische Universität Dortmund, Fakultät Physik, D-44221 Dortmund, Germany*
[19]*Technische Universität Dresden, Institut für Kern- und Teilchenphysik, D-01062 Dresden, Germany*
[20]*Laboratoire Leprince-Ringuet, CNRS/IN2P3, Ecole Polytechnique, F-91128 Palaiseau, France*
[21]*University of Edinburgh, Edinburgh EH9 3JZ, United Kingdom*
[22a]*INFN Sezione di Ferraraa, I-44100 Ferrara, Italy*
[22b]*Dipartimento di Fisica, Università di Ferrarab, I-44100 Ferrara, Italy*
[23]*INFN Laboratori Nazionali di Frascati, I-00044 Frascati, Italy*
[24a]*INFN Sezione di Genova, I-16146 Genova, Italy*
[24b]*Dipartimento di Fisica, Università di Genovab, I-16146 Genova, Italy*
[25]*Indian Institute of Technology Guwahati, Guwahati, Assam, 781 039, India*
[26]*Harvard University, Cambridge, Massachusetts 02138, USA*
[27]*Harvey Mudd College, Claremont, California 91711*
[1]*Universität Heidelberg, Physikalisches Institut, Philosophenweg 12, D-69120 Heidelberg, Germany*
[29]*Humboldt-Universität zu Berlin, Institut für Physik, Newtonstr. 15, D-12489 Berlin, Germany*
[30]*Imperial College London, London, SW72 AZ, United Kingdom*
[31]*University of Iowa, Iowa City, Iowa 52242, USA*
[32]*Iowa State University, Ames, Iowa 50011-3160, USA*
[33]*Johns Hopkins University, Baltimore, Maryland 21218, USA*
[2]*Laboratoire de l'Accélérateur Linéaire, IN2P3/CNRS et Université Paris-Sud 11, Centre Scientifique d'Orsay, B. P. 34, F-91898 Orsay Cedex, France*
[35]*Lawrence Livermore National Laboratory, Livermore, California 94550, USA*
[36]*University of Liverpool, Liverpool L697 ZE, United Kingdom*
[37]*Queen Mary, University of London, London, E14 NS, United Kingdom*
[38]*University of London, Royal Holloway and Bedford New College, Egham, Surrey TW200 EX, United Kingdom*
[39]*University of Louisville, Louisville, Kentucky 40292, USA*
[3]*Johannes Gutenberg-Universität Mainz, Institut für Kernphysik, D-55099 Mainz, Germany*
[41]*University of Manchester, Manchester M139 PL, United Kingdom*
[42]*University of Maryland, College Park, Maryland 20742, USA*
[43]*University of Massachusetts, Amherst, Massachusetts 01003, USA*
[44]*Massachusetts Institute of Technology, Laboratory for Nuclear Science, Cambridge, Massachusetts 02139, USA*
[45]*McGill University, Montréal, Québec, Canada H3A2 T8*

^{46a}INFN Sezione di Milanoa, I-20133 Milano, Italy
^{46b}Dipartimento di Fisica, Università di Milanob, I-20133 Milano, Italy
^{47}University of Mississippi, University, Mississippi 38677, USA 3
^{4}Université de Montréal, Physique des Particules, Montréal, Québec, Canada H3C3 J7
^{49a}INFN Sezione di Napolia, I-80126 Napoli, Italy
^{49b}Dipartimento di Scienze Fisiche, Università di Napoli Federico IIb, I-80126 Napoli, Italy
^{50}NIKHEF, National Institute for Nuclear Physics and High Energy Physics, NL-1009 DB Amsterdam, The Netherlands
^{51}University of Notre Dame, Notre Dame, Indiana 46556, USA
^{52}Ohio State University, Columbus, Ohio 43210, USA
^{53}University of Oregon, Eugene, Oregon 97403, USA
^{54a}INFN Sezione di Padovaa, I-35131 Padova, Italy
^{54b}Dipartimento di Fisica, Università di Padovab, I-35131 Padova, Italy
^{55}Laboratoire de Physique Nucléaire et de Hautes Energies, IN2P3/CNRS, Université Pierre et Marie Curie-Paris6,
Université Denis Diderot-Paris7, F-75252 Paris, France
^{56a}INFN Sezione di Perugiaa, I-06100 Perugia, Italy
^{56b}Dipartimento di Fisica, Università di Perugiab, I-06100 Perugia, Italy
^{57a}INFN Sezione di Pisaa, I-56127 Pisa, Italy
^{57b}Dipartimento di Fisica, Università di Pisab, I-56127 Pisa, Italy
^{57c}Scuola Normale Superiore di Pisac, I-56127 Pisa, Italy
^{58}Princeton University, Princeton, New Jersey 08544, USA
^{59a}INFN Sezione di Romaa, I-00185 Roma, Italy
^{59b}Dipartimento di Fisica, Università di Roma La Sapienzab, I-00185 Roma, Italy
^{60}Universität Rostock, D-18051 Rostock, Germany
^{61}Rutherford Appleton Laboratory, Chilton, Didcot, Oxon, OX110 QX, United Kingdom
^{62}CEA, Irfu, SPP, Centre de Saclay, F-91191 Gif-sur-Yvette, France
^{63}SLAC National Accelerator Laboratory, Stanford, California 94309 USA
^{64}University of South Carolina, Columbia, South Carolina 29208, USA
^{65}Southern Methodist University, Dallas, Texas 75275, USA
^{66}Stanford University, Stanford, California 94305-4060, USA
^{67}State University of New York, Albany, New York 12222, USA
^{68}Tel Aviv University, School of Physics and Astronomy, Tel Aviv, 69978, Israel
^{69}University of Tennessee, Knoxville, Tennessee 37996, USA
^{70}University of Texas at Austin, Austin, Texas 78712, USA
^{71}University of Texas at Dallas, Richardson, Texas 75083, USA
^{72a}INFN Sezione di Torinoa, I-10125 Torino, Italy
^{72b}Dipartimento di Fisica Sperimentale, Università di Torinob, I-10125 Torino, Italy
^{73a}INFN Sezione di Triestea, I-34127 Trieste, Italy
^{73b}Dipartimento di Fisica, Università di Triesteb, I-34127 Trieste, Italy
^{74}IFIC, Universitat de Valencia-CSIC, E-46071 Valencia, Spain
^{75}University of Victoria, Victoria, British Columbia, Canada V8W3 P6
^{76}Department of Physics, University of Warwick, Coventry CV47 AL, United Kingdom
^{77}University of Wisconsin, Madison, Wisconsin 53706, USA

Using a sample of 122×10^6 $\Upsilon(3S)$ events recorded with the *BABAR* detector at the PEP-II asymmetric-energy e^+e^- collider at SLAC, we search for the $h_b(1P)$ spin-singlet partner of the P-wave $\chi_{bJ}(1P)$ states in the sequential decay $\Upsilon(3S) \rightarrow \pi^0 h_b(1P)$, $h_b(1P) \rightarrow \gamma \eta_b(1S)$. We observe an excess of events above background in the distribution of the recoil mass against the π^0 at mass $9902 \pm 4(\text{stat}) \pm 2(\text{syst})$ MeV/c^2. The width of the observed signal is consistent with experimental resolution, and its significance is 3.1σ, including systematic uncertainties. We obtain the value $(4.3 \pm 1.1(\text{stat}) \pm 0.9(\text{syst})) \times 10^{-4}$ for the product branching fraction $\mathcal{B}(\Upsilon(3S) \rightarrow \pi^0 h_b) \times \mathcal{B}(h_b \rightarrow \gamma \eta_b)$.

---

*Now at Temple University, Philadelphia, PA 19122, USA
†Also with Università di Perugia, Dipartimento di Fisica, Perugia, Italy
‡Now at University of South Alabama, Mobile, AL 36688, USA
§Also with Università di Sassari, Sassari, Italy

To understand the spin dependence of $q\bar{q}$ potentials for heavy quarks, it is essential to measure the hyperfine mass splitting for P-wave states. In the nonrelativistic approximation, the hyperfine splitting is proportional to the square of the wave function at the origin, which is expected to be nonzero only for $L = 0$, where L is the orbital angular

momentum of the $q\bar{q}$ system. For $L = 1$, the splitting between the spin-singlet ($^1P_1$) and the spin-averaged triplet state ($\langle^3P_J\rangle$) is expected to be $\Delta M_{HF} = M(\langle^3P_J\rangle) - M(^1P_1) \sim 0$. The $^1P_1$ state of bottomonium, the $h_b(1P)$, is the axial vector partner of the P-wave $\chi_{bJ}(1P)$ states. Its expected mass, computed as the spin-weighted center of gravity of the $\chi_{bJ}(1P)$ states, is 9899.87 ± 0.27 MeV/c^2 [1]. Higher-order corrections might cause a small deviation from this value, but a hyperfine splitting larger than 1 MeV/c^2 might be indicative of a vector component in the confinement potential [2]. The hyperfine splitting for the charmonium $^1P_1$ state h_c is measured by the BES and CLEO experiments [3–5] to be ~ 0.1 MeV/c^2. An even smaller splitting is expected for the much heavier bottomonium system [2].

The $h_b(1P)$ state is expected to be produced in $\Upsilon(3S)$ decay via π^0 or di-pion emission, and to undergo a subsequent $E1$ transition to the $\eta_b(1S)$, with branching fraction (BF) $\mathcal{B}(h_b(1P) \rightarrow \gamma\eta_b(1S)) \sim (40\text{–}50)\%$ [2,6]. The isospin-violating decay $\Upsilon(3S) \rightarrow \pi^0 h_b(1P)$ is expected to have a BF of about 0.1% [7,8], while theoretical predictions for the transition $\Upsilon(3S) \rightarrow \pi^+\pi^- h_b(1P)$ range from $\sim 10^{-4}$ [7] up to $\sim 10^{-3}$ [9]. A search for the latter decay process in *BABAR* data yielded an upper limit on the BF of 1.2×10^{-4} at 90% confidence level (C.L.) [10]. The CLEO experiment reported the 90% C.L. limit $\mathcal{B}(\Upsilon(3S) \rightarrow \pi^0 h_b(1P)) < 0.27\%$, assuming the mass of the h_b to be 9900 MeV/c^2 [11].

In this paper, we report evidence for the $h_b(1P)$ state in the decay $\Upsilon(3S) \rightarrow \pi^0 h_b(1P)$. The data sample used was collected with the *BABAR* detector [12] at the PEP-II asymmetric-energy e^+e^- collider at SLAC, and corresponds to 28 fb^{-1} of integrated luminosity at a center-of-mass (CM) energy of 10.355 GeV, the mass of the $\Upsilon(3S)$ resonance. This sample contains (122 ± 1) million $\Upsilon(3S)$ events. Detailed Monte Carlo (MC) simulations [13] of samples of exclusive $\Upsilon(3S) \rightarrow \pi^0 h_b(1P)$, $h_b(1P) \rightarrow \gamma\eta_b(1S)$ decays (where the $h_b(1P)$ and $\eta_b(1S)$ are hereafter referred to as the h_b and the η_b), and of inclusive $\Upsilon(3S)$ decays, are used in this study. These samples correspond to 34 000 signal and 215×10^6 $\Upsilon(3S)$ events, respectively. In the inclusive $\Upsilon(3S)$ MC sample a BF of 0.1% is assumed for the decay $\Upsilon(3S) \rightarrow \pi^0 h_b$ [7].

The trajectories of charged particles are reconstructed using a combination of five layers of double-sided silicon strip detectors and a 40-layer drift chamber, both operating inside the 1.5-T magnetic field of a superconducting solenoid. Photons are detected, and their energies measured, with a CsI(Tl) electromagnetic calorimeter, also located inside the solenoid. The *BABAR* detector is described in detail elsewhere [12].

The signal for $\Upsilon(3S) \rightarrow \pi^0 h_b$ decays is extracted from a fit to the inclusive recoil mass distribution against the π^0 candidates ($m_{recoil}(\pi^0)$). It is expected to appear as a small excess centered near 9.9 GeV/c^2 on top of the very large

nonpeaking background produced from continuum events ($e^+e^- \rightarrow q\bar{q}$ with $q = u, d, s, c$) and bottomonium decays. The recoil mass, $m_{recoil}(\pi^0) = \sqrt{(E^*_{beam} - E^*(\pi^0))^2 - p^*(\pi^0)^2}$, where E^*_{beam} is the total beam CM energy, and $E^*(\pi^0)$ and $p^*(\pi^0)$ are the energy and momentum of the π^0, respectively, computed in the e^+e^- CM frame (denoted by the asterisk). The search for an h_b signal, requiring detection only of the recoil π^0, proved unfruitful because of the extremely large associated π^0 background encountered. In order to reduce this background significantly, we exploit the fact that the h_b should decay about half of the time [2,6] to $\gamma\eta_b$, and so require in addition the detection of a photon consistent with this decay. The precise measurement of the η_b mass [14] defines a restricted energy range for a photon candidate compatible with this subsequent h_b decay. The resulting decrease in h_b signal efficiency is offset by reduction of the π^0 background by a factor of about 20. A similar approach led to the observation by CLEO-c, and then by BES, of the h_c in the decay chain $\psi(2S) \rightarrow h_c\pi^0 \rightarrow \eta_c\gamma\pi^0$ [3–5], where the η_c was identified both exclusively (by reconstructing a large number of hadronic modes) and inclusively.

The signal photon from $h_b \rightarrow \gamma\eta_b$ decay is monochromatic in the h_b rest-frame and is expected to peak at ~ 490 MeV in the e^+e^- CM frame, with a small Doppler broadening that arises from the motion of the h_b in that frame; the corresponding energy resolution is expected to be ~ 25 MeV. The Doppler broadening is negligible compared with the energy resolution. Figure 1 shows the reconstructed CM energy distribution of candidate photons in the region 250–1000 MeV for simulated $\Upsilon(3S) \rightarrow \pi^0 h_b$, $h_b \rightarrow \gamma\eta_b$ events before the application of selection criteria; the signal photon from $h_b \rightarrow \gamma\eta_b$ decay appears as a peak on top of a smooth background. We select signal photon candidates with CM energy in the range 420–540 MeV (indicated by the shaded region in Fig. 1).
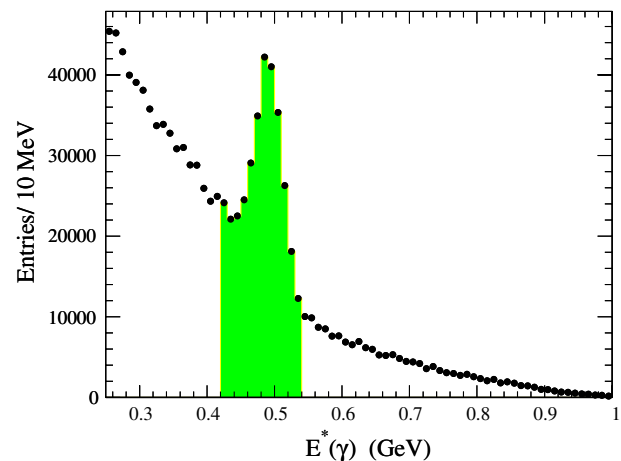

FIG. 1 (color online). The reconstructed CM energy distribution of the candidate photon in simulated $\Upsilon(3S) \rightarrow \pi^0 h_b(1P)$, $h_b(1P) \rightarrow \gamma\eta_b(1S)$ events. The shaded region indicates the selected $E^*(\gamma)$ signal region.

We employ a simple set of selection criteria to suppress backgrounds while retaining a high signal efficiency. These selection criteria are chosen by optimizing the ratio of the expected signal yield to the square root of the background. The $\Upsilon(3S) \to \pi^0 h_b$, $h_b \to \gamma \eta_b$ MC signal sample is used in the optimization, while a small fraction (9%) of the total data sample is used to model the background. We estimate the background contribution in the signal region, defined by $9.85 < m_{\text{recoil}}(\pi^0) < 9.95$ GeV/c^2, using the sidebands of the expected h_b signal region, $9.80 < m_{\text{recoil}}(\pi^0) < 9.85$ GeV/c^2 and $9.95 < m_{\text{recoil}}(\pi^0) < 10.00$ GeV/c^2.

The decay of the η_b is expected to result in high final-state track multiplicity. Therefore, we select a hadronic event candidate by requiring that it have at least four charged-particle tracks and a ratio of the second to zeroth Fox-Wolfram moments [15] less than 0.6 [16].

For a given event, we require that the well-reconstructed tracks yield a successful fit to a primary vertex within the $e^+ e^-$ collision region. We then constrain the candidate photons in that event to originate from that vertex.

A photon candidate is required to deposit a minimum energy in the laboratory frame of 50 MeV into a contiguous electromagnetic calorimeter crystal cluster that is isolated from all charged-particle tracks in that event. To ensure that the cluster shape is consistent with that for an electromagnetic shower, its lateral moment [17] is required to be less than 0.6.

A π^0 candidate is reconstructed as a photon pair with invariant mass $m(\gamma\gamma)$ in the range 55–200 MeV/c^2 (see Fig. 2). In the calculation of $m_{\text{recoil}}(\pi^0)$, the γ-pair invariant mass is constrained to the nominal π^0 value [1] in order to improve the momentum resolution of the π^0. To suppress backgrounds due to misreconstructed π^0 candidates, we require $|\cos\theta_h| < 0.7$, where the helicity angle θ_h is defined as the angle between the direction of a γ from a π^0

candidate in the π^0 rest-frame, and the π^0 direction in the laboratory.

Photons from π^0 decays are a primary source of background in the region of the signal photon line from $h_b \to \gamma \eta_b$ transitions. A signal photon candidate is rejected if, when combined with another photon in the event (γ_2), the resulting $\gamma\gamma_2$ invariant mass is within 15 MeV/c^2 of the nominal π^0 mass; this is called a π^0 veto. Similarly, many misreconstructed π^0 candidates result from the pairing of photons from different π^0's. A π^0 candidate is rejected if either of its daughter photons satisfies the π^0 veto condition, with γ_2 not the other daughter photon. To maintain high signal efficiency, the π^0 veto condition is imposed only if the energy of γ_2 in the laboratory frame is greater than 200 MeV (150 MeV) for the signal photon (for the π^0 daughters). With the application of these vetoes, and after all selection criteria have been imposed, the average π^0 candidate multiplicity per event is 2.17 for the full range of $m(\gamma\gamma)$, and 1.34 for the π^0 signal region ($110 < m(\gamma\gamma) < 150$ MeV/c^2). The average multiplicity for the signal photon is 1.02. For 98.4% of π^0 candidates there is only one associated photon candidate.

We obtain the $m_{\text{recoil}}(\pi^0)$ distribution in 90 intervals of 3 MeV/c^2 from 9.73 to 10 GeV/c^2. For each $m_{\text{recoil}}(\pi^0)$ interval, the $m(\gamma\gamma)$ spectrum consists of a π^0 signal above combinatorial background (see Fig. 2). We construct the $m_{\text{recoil}}(\pi^0)$ spectrum by extracting the π^0 signal yield in each interval of $m_{\text{recoil}}(\pi^0)$ from a fit to the $m(\gamma\gamma)$ distribution in that interval. The $m_{\text{recoil}}(\pi^0)$ distribution is thus obtained as the fitted π^0 yield and its uncertainty for each interval of $m_{\text{recoil}}(\pi^0)$.

We use the MC background and MC π^0-signal distributions directly in fitting the $m(\gamma\gamma)$ distributions in data [18]. For each $m_{\text{recoil}}(\pi^0)$ interval in MC, we obtain histograms in 0.1 MeV/c^2 intervals of $m(\gamma\gamma)$ corresponding to the π^0-signal and background distributions. The π^0-signal distribution is obtained by requiring matching of the reconstructed to the generated π^0's on a candidate-by-candidate basis (termed "truth-matching" in the following discussion). The histogram representing background is obtained by subtraction of the π^0 signal from the total distribution.

For both signal and background the qualitative changes in shape over the full range of $m_{\text{recoil}}(\pi^0)$ are quite well reproduced by the MC. However, the π^0 signal distribution in data is slightly broader than in MC, and is peaked at a slightly higher mass value. The $m(\gamma\gamma)$ background shape also differs between data and MC. To address these differences, the MC π^0 signal is displaced in mass and smeared by a double Gaussian function with different mean and width values; the MC background distribution is weighted according to a polynomial in $m(\gamma\gamma)$. The signal-shape and background-weighting parameter values are obtained from a fit to the $m(\gamma\gamma)$ distribution in data for the full range of $m_{\text{recoil}}(\pi^0)$. At each step in the fitting procedure, the π^0
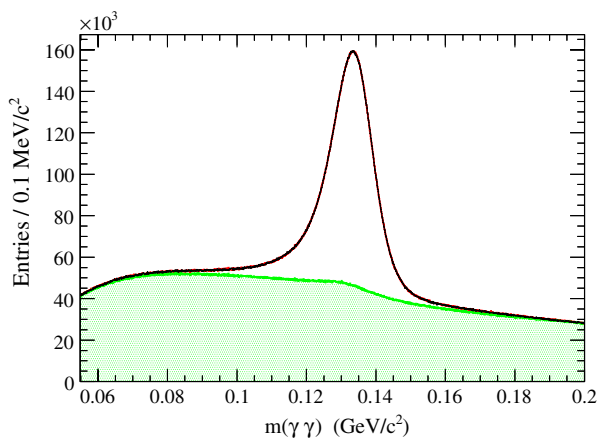

FIG. 2 (color online). The result of the fit to the $m(\gamma\gamma)$ distribution in data (data points) for the full range of $m_{\text{recoil}}(\pi^0)$. The solid histogram shows the fit result, and is essentially indistinguishable from the data; the shaded histogram corresponds to the background distribution.

signal and background distributions are normalized to unit area, and a χ^2 between a linear combination of these MC histograms and the $m(\gamma\gamma)$ distribution in data is computed. The fit function provides an excellent description of the data ($\chi^2/\mathrm{NDF} = 1446/1433$; NDF = number of degrees of freedom) and the fit result is essentially indistinguishable from the data histogram. The background distribution exhibits a small peak at the π^0 mass, due to interactions in the detector material of the type $n\pi^+ \rightarrow p\pi^0$ or $p\pi^- \rightarrow n\pi^0$ that cannot be truth-matched. The normalization of this background to the nonpeaking background is obtained from the MC simulation, which incorporates the results of detailed studies of interactions in the detector material performed using data [20]. This peak is displaced and smeared as for the primary π^0 signal.

The fits to the individual $m(\gamma\gamma)$ distributions are performed with the smearing and weighting parameters fixed to the values obtained from the fit shown in Fig. 2. In this process, the MC signal and background distributions for each $m_{\mathrm{recoil}}(\pi^0)$ interval are shifted, smeared, and weighted using the fixed parameter values, and then normalized to unit area. Thus, only the signal and background yields are free parameters in each fit. The χ^2 fit to the data then gives the value and the uncertainty of the number of π^0 events in each m_{recoil} interval. The fits to the 90 $m(\gamma\gamma)$ distributions provide good descriptions of the data, with an average value of $\langle \chi^2/\mathrm{NDF} \rangle = 0.98$ (NDF = 1448), and r.m.s. deviation of 0.03 for the distribution of values. We verify that the fitted π^0 yield is consistent with the number of truth-matched π^0's in MC to ensure that the π^0 selection efficiency is well-determined, and to check the validity of the π^0 signal-extraction procedure.

To search for an h_b signal, we perform a binned χ^2 fit to the $m_{\mathrm{recoil}}(\pi^0)$ distribution obtained in data. The h_b signal function is represented by the sum of two Crystal Ball functions [19] with parameter values, other than the h_b mass, m, and the normalization, determined from simulated signal $\Upsilon(3S) \rightarrow \pi^0 h_b$ events. The background is well represented with a fifth-order polynomial function.

Direct MC simulation fails to yield an adequate description of the observed background distribution, although the overall shape is similar in data and MC. This is due primarily to the complete absence of experimental information on the decay modes of the h_b and η_b mesons. Simulation studies with a background component that is weighted to accurately model the distribution in data show a negative bias of $\sim35\%$ in the signal yield from a procedure in which the background shape and signal mass and yield are determined simultaneously in the fit. Consequently, we define a region of $m_{\mathrm{recoil}}(\pi^0)$ chosen as the signal interval based on the expected mass value and signal resolution. The signal region includes any reasonable theoretical expectation for the h_b mass. We fit the $m_{\mathrm{recoil}}(\pi^0)$ background distribution outside the signal interval and interpolate the background to

the signal region to obtain an estimate of its uncertainty therein. Figure 3(a) shows the result of the fit to the distribution of $m_{\mathrm{recoil}}(\pi^0)$ in data excluding the signal region, $9.87 \leq m_{\mathrm{recoil}}(\pi^0) \leq 9.93$ GeV/c^2. The fit yields $\chi^2/\mathrm{NDF} = 50.8/64$, and the result is represented by the histogram in Fig. 3(a), including the interpolation to the h_b signal region.

We then perform a fit over the 20 intervals of the signal region to search for an h_b signal of the expected shape. We take account of the correlated uncertainties related to the polynomial interpolation procedure by creating a 20×20 covariance matrix using the 6×6 covariance matrix which results from the polynomial fit. The error matrix for the signal region, E, is obtained by adding the diagonal 20×20 matrix of squared error values from the $m_{\mathrm{recoil}}(\pi^0)$ distribution, and a χ^2 value is defined by
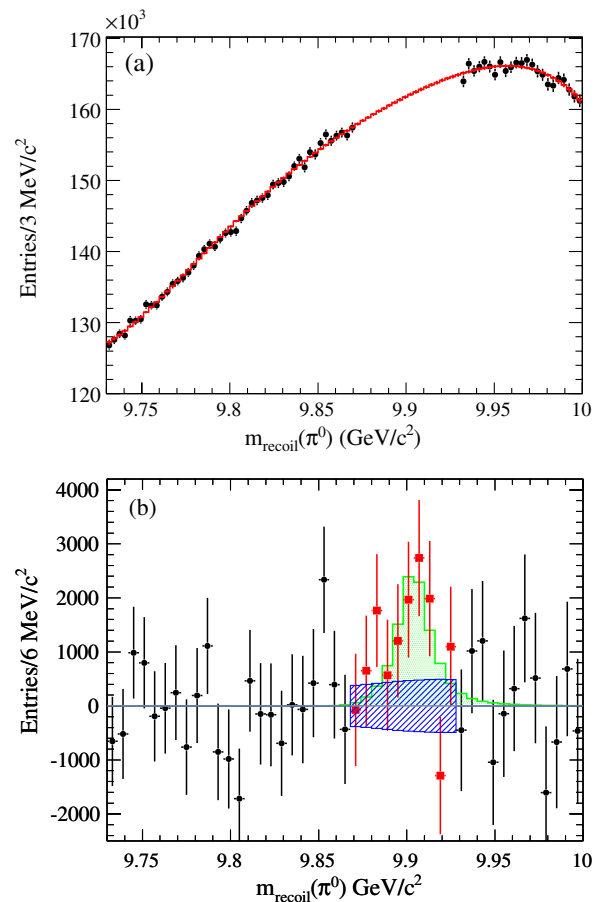

FIG. 3 (color online). (a) The $m_{\mathrm{recoil}}(\pi^0)$ distribution in the region $9.73 < m_{\mathrm{recoil}}(\pi^0) < 10$ GeV/c^2 for data (points); the solid histogram represents the fit function described in the text. The data in the h_b signal region have been excluded from the fit and the plot. (b) The $m_{\mathrm{recoil}}(\pi^0)$ spectrum after subtracting background; in the h_b signal region the data points are shown as squares, and the area with diagonal shading represents the uncertainties from the background fit; the shaded histogram represents the signal function resulting from the fit to the data.

$$\chi^2 = \tilde{V}E^{-1}V. \quad (1)$$

Here V is the column vector consisting of the difference between the measured value of the $m_{\mathrm{recoil}}(\pi^0)$ distribution and the corresponding sum of the value of the background polynomial and that of the h_b signal function for each of the 20 3 MeV/c^2 intervals in the signal region. In Fig. 3(b) we plot the difference between the distribution of $m_{\mathrm{recoil}}(\pi^0)$ and the fitted histogram of Fig. 3(a) over the entire region from 9.73 GeV/c^2 to 10.00 GeV/c^2; we have combined pairs of 3 MeV/c^2 intervals from Fig. 3(a) for clarity. The yield obtained from the fit to the signal region is 10814 ± 2813 events and the h_b mass value obtained is $m = 9902 \pm 4$ MeV/c^2 with a χ^2 value of 14.7 for 18 degrees of freedom.

In order to determine the statistical significance of the signal we repeat the fit with the h_b mass fixed to the spin-weighted center of gravity of the $\chi_{bJ}(1P)$ states, $m = 9900$ MeV/c^2. The signal yield obtained from the fit is 10721 ± 2806. The statistical significance of the signal, calculated from the square-root of the difference in χ^2 for this fit with and without a signal component, is 3.8 standard deviations, in good agreement with the signal size obtained.

Fit validation studies were performed. No evidence of bias is observed in large MC samples with simulated h_b mass at 9880, 9900, and 9920 MeV/c^2. In addition, the result of a scan performed in data as a function of the assumed h_b mass indicates that the preferred peak position for the signal is at 9900 MeV/c^2, in excellent agreement with the result of Fig. 3(b).

We obtain an estimate of systematic uncertainty on the number of π^0's in each $m_{\mathrm{recoil}}(\pi^0)$ interval by repeating the fits to the individual $m(\gamma\gamma)$ spectra with the line shape parameters corresponding to Fig. 2 varied within their uncertainties. The distribution of the net uncertainty varies as a third-order polynomial in $m_{\mathrm{recoil}}(\pi^0)$. We estimate a systematic uncertainty of ±210 events on the h_b signal yield due to the π^0-yield extraction procedure by evaluating this function at the fitted h_b mass value.

The dominant sources of systematic uncertainty on the measured h_b yield are the order of the polynomial describing the $m_{\mathrm{recoil}}(\pi^0)$ background distribution, and the width of the h_b signal region. By varying the polynomial from fifth to seventh order, and by expanding the region excluded from the fit in Fig. 3(a) from (9.87–9.93) GeV/c^2 to (9.85–9.95) GeV/c^2, we obtain systematic uncertainties of ±1065 events and ±1263 events, respectively, taken from the full excursions of the h_b yield under these changes. Similarly, we obtain a total systematic uncertainty of ±1.5 MeV/c^2 on the h_b mass due to the choice of background shape.

The systematic uncertainty associated with the choice of signal line shape is estimated by varying the signal function parameters, which were fixed in the fit, by ±1σ. We assign the largest deviation from the nominal fit result as a systematic error. Systematic uncertainties of ±154 events

and ±0.3 MeV/c^2 are obtained for the h_b yield and mass, respectively.

After combining these systematic uncertainty estimates in quadrature, we obtain an effective signal significance of 3.3 standard deviations. The smallest value of the significance among those calculated for the varied fits in the systematics study is 3.1 standard deviations. The h_b yield is 10814 ± 2813 ± 1652 events and the h_b mass value $m = 9902 \pm 4 \pm 2$ MeV/c^2, where the first uncertainty is statistical and the second systematic. The resulting hyperfine splitting with respect to the center of gravity of the $\chi_{bJ}(1P)$ states is thus $\Delta M_{\mathrm{HF}} = +2 \pm 4 \pm 2$ MeV/c^2, which agrees within error with model predictions [7,8].

To convert the h_b signal yield into a measurement of the product BF for the sequential decay $\Upsilon(3S) \to \pi^0 h_b$, $h_b \to \gamma\eta_b$, we determine the efficiency ϵ_S from MC by requiring that the signal π^0 and the γ be truth-matched. The resulting efficiency is $\epsilon_S = 15.8 \pm 0.2\%$. Monte Carlo studies indicate that photons that are not from an $h_b \to \gamma\eta_b$ transition can satisfy the selection criteria when only the $\Upsilon(3S) \to \pi^0 h_b$ transition is truth-matched. This causes a fictitious increase in the h_b signal efficiency to $\epsilon = 17.9 \pm 0.2\%$. Therefore, the efficiency for observed h_b signal events that do not correspond to $h_b \to \gamma\eta_b$ decay is $\Delta\epsilon = 2.1\%$. However, there is no current experimental information on the production of such nonsignal photons in h_b and η_b decays. Furthermore, the above estimate of efficiencies in MC does not account for photons from hadronic h_b decays, since the signal MC requires $h_b \to \gamma\eta_b$. We thus assume that random photons from hadronic h_b decays have the same probability $\Delta\epsilon$ to satisfy the signal photon selection criteria as those from η_b decays. We assume a 100% uncertainty on the value of $\Delta\epsilon$ when estimating the systematic error on the product BF.

We estimate the product BF for $\Upsilon(3S) \to \pi^0 h_b$, $h_b \to \gamma\eta_b$ by dividing the fitted signal yield, N, corrected for the estimated total reconstruction efficiency, by the number of $\Upsilon(3S)$ events, $N_{\Upsilon(3S)}$, in the data sample. We obtain the following expression for the product BF:

$$\mathcal{B}(\Upsilon(3S) \to \pi^0 h_b) \times \mathcal{B}(h_b \to \gamma\eta_b) = \frac{N}{N_{\Upsilon(3S)}\epsilon_S} \cdot \frac{1}{C}, \quad (2)$$

where

$$C = 1 + \frac{\Delta\epsilon}{\epsilon_S} \cdot \frac{1}{\mathcal{B}(h_b \to \gamma\eta_b)} \quad (3)$$

is the factor that corrects the efficiency ϵ_S for the nonsignal hadronic h_b and η_b contributions. In this equation, we assume a BF value $\mathcal{B}(h_b \to \gamma\eta_b) = 45 \pm 5\%$ according to the current range of theoretical predictions. The corresponding correction factor is $1 - C \sim 30\%$, with a systematic uncertainty dominated by the uncertainty on $\Delta\epsilon$.

We obtain $\mathcal{B}(\Upsilon(3S) \to \pi^0 h_b) \times \mathcal{B}(h_b \to \gamma\eta_b) = (4.3 \pm 1.1 \pm 0.9) \times 10^{-4}$, where the first uncertainty is

statistical and the second systematic. The result is consistent with the prediction of Ref. [8], which estimates 4×10^{-4} for the product BF. Since the h_b-decay uncertainty reduces the significance of the product BF relative to that of the h_b production, we may also quote an upper limit on the product BF. From an ensemble of simulated events using the measured product BF value, and the statistical and associated systematic uncertainties (assumed to be Gaussian) as input, we obtain $\mathcal{B}(\Upsilon(3S) \rightarrow \pi^0 h_b) \times \mathcal{B}(h_b \rightarrow \gamma \eta_b) < 6.1 \times 10^{-4}$ at 90% C.L.

In summary, we have found evidence for the decay $\Upsilon(3S) \rightarrow \pi^0 h_b$, with a significance of at least 3.1 standard deviations, including systematic uncertainties. The measured mass value, $m = 9902 \pm 4(\text{stat}) \pm 2(\text{syst})$ MeV/c^2, is consistent with the expectation for the $h_b(1P)$ bottomonium state [2,21], the axial vector partner of the $\chi_{bJ}(1P)$ triplet of states. We obtain $\mathcal{B}(\Upsilon(3S) \rightarrow \pi^0 h_b) \times \mathcal{B}(h_b \rightarrow \gamma \eta_b) = (4.3 \pm 1.1(\text{stat}) \pm 0.9(\text{syst})) \times 10^{-4}$ ($< 6.1 \times 10^{-4}$ at 90% C.L.).

Note added in proof.—After this paper was submitted, preliminary results of a search for the h_b in the reaction $e^+ e^- \rightarrow h_b(nP)\pi^+\pi^-$ in data collected near the $\Upsilon(5S)$ resonance have been announced by the Belle Collaboration [22]. The $h_b(1P)$ mass measured therein agrees very well with the value reported in this paper.

[1] K. Nakamura *et al.* (Particle Data Group), J. Phys. G **37,** 075021 (2010).

[2] S. Godfrey and J. L. Rosner, Phys. Rev. D **66,** 014012 (2002).

[3] M. Ablikim *et al.* (BES Collaboration), Phys. Rev. Lett. **104,** 132002 (2010).

[4] J. L. Rosner *et al.* (CLEO Collaboration), Phys. Rev. Lett. **95,** 102003 (2005); S. Dobbs *et al.* (CLEO Collaboration), Phys. Rev. Lett. **101,** 182003 (2008).

[5] G. S. Adams *et al.* (CLEO Collaboration), Phys. Rev. D **80,** 051106 (2009).

[6] J. L. Rosner *et al.* (CLEO Collaboration), Phys. Rev. Lett. **95,** 102003 (2005).

[7] M. B. Voloshin, Sov. J. Nucl. Phys. **43,** 1011 (1986).

[8] S. Godfrey, J. Phys. Conf. Ser. **9,** 123 (2005).

[9] Y. P. Kuang and T. M. Yan, Phys. Rev. D **24,** 2874 (1981); Y. P. Kuang, S. F. Tuan, and T. M. Yan, Phys. Rev. D **37,** 1210 (1988); Y. P. Kuang and T. M. Yan, Phys. Rev. D **41,** 155 (1990); S. F. Tuan, Mod. Phys. Lett. A **7,** 3527 (1992).

[10] J. P. Lees *et al.* (BABAR Collaboration), Phys. Rev. D **84,** 011104(R) (2011).

[11] F. Butler *et al.* (CLEO Collaboration), Phys. Rev. D **49,** 40 (1994).

[12] B. Aubert *et al.* (BABAR Collaboration), Nucl. Instrum. Methods Phys. Res., Sect. A **479,** 1 (2002).

[13] The MC events are generated using the JETSET 7.4 and PYTHIA programs to describe the hadronization process from the Lund string fragmentation model with final-state radiation included.

[14] B. Aubert *et al.* (BABAR Collaboration), Phys. Rev. Lett. **101,** 071801 (2008); **102,** 029901(E) (2009).

[15] G. C. Fox and S. Wolfram, Nucl. Phys. **B149,** 413 (1979).

[16] This quantity is indicative of the collimation of an event topology, with values close to 1 for jetlike events; the kinematics of a heavy object such as the η_b decaying hadronically result in a more spherical event.

[17] A. Drescher *et al.*, Nucl. Instrum. Methods Phys. Res., Sect. A **237,** 464 (1985).

[18] In MC simulations, fits to the individual $m(\gamma\gamma)$ spectra that make use of a polynomial background function and various combinations of Crystal Ball [19] and/or Gaussian signal functions proved unsatisfactory at the high statistical precision necessary.

[19] M. J. Oreglia, Ph.D. thesis, Report No. SLAC-R-236, 1980; J. E. Gaiser, Ph.D. thesis, Report No. SLAC-R-255, 1982; T. Skwarnicki, Ph.D. thesis, Report No. DESY F31-86-02, 1986.

[20] S. Agostinelli *et al.* (Geant4 Collaboration), Nucl. Instrum. Methods Phys. Res., Sect. A **506,** 250 (2003); T. Sjöstrand and M. Bengtsson, Comput. Phys. Commun. **43,** 367 (1987).

[21] S. Meinel, Phys. Rev. D **82,** 114502 (2010).

[22] I. Adachi *et al.* (Belle Collaboration), arXiv:1103.3419v1.